Laboratory Investigation (2005) 85, 608–623

www.laboratoryinvestigation.org

VEGF contributes to mammary tumor growth in transgenic mice through paracrine and autocrine mechanisms

Daniel J Schoeffner[1], Shannon L Matheny[1], Takemi Akahane[1], Valentina Factor[2], Adam Berry[1], Glenn Merlino[3] and Unnur P Thorgeirsson[1]

[1]*Laboratory of Cellular Carcinogenesis and Tumor Promotion, Center for Cancer Research, National Cancer Institute, National Institutes of Health, Bethesda, MD, USA;* [2]*Laboratory of Experimental Carcinogenesis, Center for Cancer Research, National Cancer Institute, National Institutes of Health, Bethesda, MD, USA and* [3]*Laboratory of Molecular Biology, Center for Cancer Research, National Cancer Institute, National Institutes of Health, Bethesda, MD, USA*

Vascular endothelial growth factor (VEGF) has been identified as a vascular permeability factor, angiogenic cytokine, and a survival factor. To address its role in mammary carcinogenesis, we used transgenic mice with human $VEGF_{165}$ targeted to mammary epithelial cells under the control of the mouse mammary tumor virus (MMTV) promoter. Metastatic mammary carcinomas were induced by mating the MMTV-VEGF mice with MMTV-polyoma virus middle T-antigen (MT) mice to generate VEGF/MT mice. Tumor latency was decreased in the VEGF/MT mice, which developed mammary carcinomas with increased vasodilatation at 4 weeks of age. There was increased incidence, multiplicity, and weight of the mammary tumors in 6- and 8-week-old VEGF/MT mice, compared to their MT-only littermates. Macro- and microscopic lung metastases were detected in the VEGF/MT mice but not the MT mice at 6 and 8 weeks of age. Enhanced tumor growth was attributed to increased microvascular density (MVD), as well as increased tumor cell proliferation and survival. Angiogenesis array analysis showed that 24 of 25 differentially expressed genes were upregulated in the VEGF/MT tumors. *In vitro* studies revealed increased proliferative activity and upregulation of Flk-1 in the VEGF/MT tumor cells, compared with the MT-only tumor cells. Moreover, there was decreased proliferative activity with down-regulation of Flk-1 in tumor cells isolated from conditional knockout ($VEGF^{-/-}$) MT-induced mammary carcinomas. The slow growing $VEGF^{-/-}$ tumor cells were accumulated in the G_1/G_0 phase of the cell cycle and this was associated with stimulation of $p16^{ink4a}$ and $p21^{WAF1}$. Similarly, $p16^{ink4a}$ was stimulated in $VEGF^{lox/lox}$/MT mammary tumor cells following Adeno-cre-mediated VEGF gene inactivation. Collectively, the data from these transgenic models indicate that VEGF contributes to mammary tumor growth through increased neovascularization, as well as autocrine stimulation of growth and inhibition of apoptosis.
Laboratory Investigation (2005) **85,** 608–623, advance online publication, 14 March 2005; doi:10.1038/labinvest.3700258

Keywords: VEGF; mammary; transgenic; middle T; growth; Flk-1

Angiogenesis is essential for development, reproduction, and wound healing. When the regulatory control is lost, angiogenesis can contribute to numerous pathological conditions such as rheumatoid arthritis, neovascular disorders, and tumorigenesis. Folkman [in 1971][1,2] first introduced the hypothesis that tumor growth is angiogenesis-dependent. This hypothesis has been supported by numerous lines of evidence suggesting that angiogenesis allows for almost exponential growth of tumor cell populations. Angiogenesis is also an essential component of tumor metastasis.[3] The extent of angiogenesis, as determined by measurement of microvascular density (MVD), is significantly associated with overexpression of Vascular endothelial growth factor (VEGF).[4] VEGF is overexpressed in human breast cancer[5] and is an independent indicator of relapse-free and overall survival in node-negative breast cancer.[6]

VEGF was first discovered as a potent vascular permeability factor,[7] and subsequently as a vascular endothelial cell mitogen[8] and a survival factor,[9] It is a ligand for the tyrosine kinase receptors, Flt-1, Flk-1/KDR, and the $VEGF_{165}$ isoform-specific receptor,

Correspondence: Dr UP Thorgeirsson, MD, Laboratory of Cellular Carcinogenesis and Tumor Promotion, Center for Cancer Research, National Cancer Institute, National Institutes of Health, Bldg. 37, Room 4032A, 9000 Rockville Pike, Bethesda, MD 20892, USA.
E-mail: thorgeiu@mail.nih.gov
Received 20 October 2004; revised 6 January 2005; accepted 13 January 2005; published online 14 March 2005

neuropilin-1 ((Nrp-1).[10,11] A critical role of VEGF receptor signaling in blood vessel development was confirmed through targeted disruptions of VEGF or its cognate receptors in mice. Embryos lacking a single allele of VEGF displayed abnormal blood vessel development and lethality.[12] Also, homozygous deletion of Flt-1 or Flk-1 prevented normal vascularization and embryonic development.[13,14]

Initially, VEGF was believed to act exclusively on endothelial cells. Later, it was found to stimulate migration, proliferation, and survival of nonendothelial cells, including monocytes,[15] neurons,[16] chondrocytes,[17] retinal epithelium,[18] and smooth muscle cells.[19] The identification of VEGF receptor expression in carcinoma cell lines[20–22] and in a variety of solid tumors[23–25] has generated interest in proposed autocrine functions of VEGF in cancer. To evaluate the effects of VEGF on mammary carcinogenesis and metastasis, we used transgenic mice with targeted expression of $hVEGF_{165}$ or MMTV-polyoma virus middle T-antigen (MT) to mammary epithelial cells through the use of the mouse mammary tumor virus (MMTV) promoter. The MT mouse has been shown to be valuable for the study of multistep progression of mammary lesions to malignancy and metastasis.[26,27]

Materials and methods

Generation of MMV-VEGF Transgenic Mice

Judy Abraham (California Biotechnology) kindly provided human $VEGF_{165}$ ($hVEGF_{165}$) used in the construction of the MMTV-VEGF (VEGF) transgenic mouse line. *Bam*HI was employed to release a 605 bp fragment containing the coding sequence, which was cloned into the expression vector pSKMMTV-SVPA (provided by Randall Moreadith). This vector contained the MMTV-LTR promoter, derived from plasmid pA9,[28] as well as the SV40 polyadenylation site and the splicing signal. The plasmid LA790 (obtained from Bill LaRochelle) was the source of the 4.7 kb *Xho*I–*Spe*I expression fragment, which was used for microinjection into FVB single-cell embryos as described by Jhappan *et al*[29] None of the founders showed phenotypic abnormalities. The founder (MV15) with the highest VEGF expression in mammary glands was selected to generate all subsequent mice for the mammary carcinogenesis study. The MMTV-MT (MT) mice were kindly provided by William J Muller (McMaster University). They develop spontaneous metastatic mammary carcinomas and have been described in detail by Guy *et al*.[26] The VEGF and MT transgenic mouse lines were maintained as hemizygotes through brother-sister mating on a FVB/N background. They were crossed to create the double transgenic VEGF/MT line. Subsequent breeding within this new line involved the mating of a hemizygous VEGF female with a hemizygous MT male. The transgenes were passed in a Mendelian fashion with the resulting genotypes as follows: wildtype (WT); VEGF single transgenic; MT single transgenic; and VEGF/MT double transgenic. Transgenic offsprings were identified by PCR analysis of genomic DNA from tail clippings, using transgene-specific primers. All animals were cared for and maintained in accordance with the National Institutes of Health (NIH) animal care guidelines. The development of mammary carcinomas with VEGF gene inactivation ($VEGF^{-/-}$) was accomplished through mating of $MMTV\text{-}MT/VEGF^{lox/lox}$ mice with $MMTV\text{-}Cre/VEGF^{lox/lox}$ mice. The VEGF Lox mice were provided by Napoleone Ferrara (Genentech) and the MMTV-Cre mice by Lothar Hennighausen (NIDDK, NIH). Of the 24 offsprings produced by the eight mating pairs used, only one tumor-bearing female displayed the $VEGF^{-/-}$ genotype. Therefore, a tumorigenesis study could not be performed. Palpable mammary tumors were first detected in the $VEGF^{-/-}$ mouse at 6 months of age. The mouse was euthanized at nine months of age and had six mammary tumors, three of which were of sufficient size for obtaining samples.

Sample Collection and Mammary Gland Whole-Mount Preparation

All mice used in the tumor study were killed according to the NIH animal care guidelines. Blood was collected in serum-separation tubes (SST®, Becton-Dickerson, Franklin Lake, NJ, USA USA), held on ice for 30 min, and then centrifuged at 1500 *g* for 25 min. The serum samples were stored at −70°C until analyzed for mouse and transgenic human VEGF levels. All tumors were excised, weighed, and rinsed in phosphate-buffered saline (PBS). Tumors arising in the right and left inguinal mammary glands (R4, L4) of the VEGF overexpressing mice were used for RNA isolation and immunohistochemistry. Three of the $VEGF^{-/-}$ tumors were used for histology and RNA isolation. In addition, two of the three $VEGF^{-/-}$ tumors were of sufficient size to also allow harvesting of tumor cells for *in vitro* studies. Samples destined for immediate RNA analysis were placed in RNA*later*™ (Ambion, Austin, TX, USA); others were snap-frozen in liquid nitrogen. Tissues for immunohistochemistry were either fixed in 10% buffered formalin or placed in Tissue-Tek® O.C.T.™ compound (Sakura, Torrance, CA, USA) and frozen in a 2-methylbutane/dry ice slurry. The lungs of all tumor-bearing mice were inflated *in situ* through the trachea, using 10% buffered formalin. Four hemotoxylin and eosin (H&E)-stained cross-sections of the lungs, cut 50 μm apart, were used to enumerate micro- and macrometastases.

For mammary gland whole-mount preparations, the inguinal mammary glands were surgically removed and spread on glass microscope slides. After fixation in Carnoy's solution, the glands were

hydrated and stained with Carmine Red, dehydrated, and mounted as described previously.[30] Mammary glands, excised from 4-week-old MT and VEGF/MT mice for visualization of the vascular tree, were processed according to the whole-mount procedure described above with the following modifications: mice were anesthetized with an intraperitoneal injection of a ketamine:xylazine solution (0.5 mg/20 g body weight) and the blood vessels were cauterized prior to excision of the mammary glands. The mounted glands were fixed overnight in 2% paraformaldehyde. After processing, all whole mounts were examined using a stereomicroscope (Nikon SMZ1200) affixed with a digital camera (Nikon DXM1200) and related ACT-1 computer software.

Northern Blot Analysis and RT-PCR

Total RNA from normal tissues, tumors, and cultured cells was prepared using RNA-Bee according to the manufacturer's instructions (Tel-Test, Friendswood, TX, USA) and treated with DNA-free™ (Ambion, Austin, TX, USA) to remove contaminating DNA. Northern blot analysis was performed on 10 μg of total RNA, which was subjected to 1% formaldehyde agarose gel electrophoresis and transferred to a nylon membrane (Schleicher and Schuell, Keene, NH, USA). Membranes were rinsed in 2 $\times$ SSC, partially dried, crosslinked, and stored at -20°C until hybridized with a 391 bp fragment of the transgenic $VEGF_{165}$ construct, containing a portion of the polyA tail. Total endogenous mouse and transgenic VEGF were detected using a 352 bp fragment containing exon 1 to exon 4 of mouse VEGF. All probes were randomly labeled with ^{32}P using RediPrimeII (Amersham Biosciences, Piscataway, NJ, USA) and hybridized in Express Hybridization solution (Clontech, Palo Alto, CA, USA). The resulting bands were visualized by exposure to Hyperfilm™ MP (Amersham Biosciences, Piscataway, NJ, USA) at -70°C. For RT-PCR analysis, first-strand cDNA was synthesized from 2.5 μg of oligo(dT) primed total RNA using Superscript™ First-Strand Synthesis System (Life Technologies, Rockville, MD, USA). PCR amplification of cDNA for all fragments was performed with PCR Platinum Supermix (Life Technologies, Rockville, MD, USA) using 2 μl of the first-strand cDNA reaction and the following primers:

Gene	*Sense*	*Antisense*
β-actin	gca ttg ctg aca gga tgc ag	cct gct tgc tga tcc aca tc
CD31	gtc atg gcc atg gtc gag tac a	ttc gga ctg gca gct gat gc
CD34	gct ggg tag ctc tct gcc tga t	acc ctg ggc caa cct cac tt
Flk-1	agc ttg gct cac agg caa cat cgg	tgg ccc gct taa cgg tcc gta gg
total VEGF	ccc tcc gaa acc atg aac ttt	ggc ttt ggt gag gtt tga tcc
human VEGF	gat gag atc gag tac atc ttc	ttg gag gag tag aat gtt gag

Semiquantitative PCR analysis of first-strand cDNA was accomplished by terminating the reactions at three different cycle numbers within the logarithmic phase of amplification and normalization to β-actin. PCR apoptosis detection kit (CytoXpress™, BioSource International, Inc., Camarillo, CA, USA) was used to determine RNA expression of four apoptosis-related genes (LICE, bcl-2, bax, bcl-xL).

Angiogenesis-specific gene expression was analyzed in pooled RNA samples of MT and VEGF/MT tumors using the GEArray™ Q series mouse angiogenesis array (SuperArray, Bethesda, MD, USA). The pooled samples consisted of 5 μg of total RNA from six primary MT tumors and six VEGF/MT tumors. Prior to the pooling of the tumor samples, 2 μg of RNA were run on an agarose-formaldehyde gel to ensure RNA integrity. The pooled samples were quantitated, and analyzed by agarose-formaldehyde gel electrophoresis prior to ^{32}P labeling and hybridization according to the manufacturer's instructions.

Immunohistochemistry and VEGF Assays

To visualize tumor microvasculature, frozen, ethanol fixed, MT and VEGF/MT tumor sections were incubated overnight at 4°C with and without rat anti-mouse CD31 monoclonal antibody (BD Pharmingen, San Diego, CA, USA) at 0.5 μg/ml, followed by the use of a rat IgG VECTASTAIN® Elite ABC kit, DAB, and methyl green (all from Vector Laboratories, Burlingame, CA, USA). MVD was determined in 10 microscopic fields (magnification $\times$400) in each of five MT-only tumors and six VEGF/MT tumors, selecting the areas with the highest MVD within each tumor. Serial sections of formalin-fixed, paraffin-embedded tumor sections from nine MT and nine VEGF/MT mice were evaluated for histopathology (hemotoxylin and eosin (H&E) staining), apoptosis, proliferation, and Flk-1 expression. TumorTACS™ *In situ* Apoptosis Detection Kit (Trevigen, Gaithersburg, MD, USA) was used to detect apoptotic cells and ImmunoCruz™ proliferating cell nuclear antigen (PCNA) staining system (Santa Cruz Biotechnology, Santa Cruz, CA, USA) to detect proliferating cells. Care was taken to count exclusively apoptotic and proliferating tumor cells. The cells were counted in 15 microscopic fields per tumor at a magnification $\times$400. For immunostaining of Flk-1, sections were incubated overnight at 4°C with or without a mouse monoclonal Flk-1 antibody (A-3, 200 μg/ml) (Santa Cruz Biotechnology, Santa Cruz, CA, USA), using 2 μg/ml of the Mouse on mouse (M.O.M.) immunodetection kit, followed by goat IgG Vectastain ABC kit and incubation with DAB or NovaRed™ (all from Vector Laboratories, Burlingame, CA, USA).

Mouse and human VEGF were quantitated in serum samples, lysates of mammary glands, and

cultured tumor cells, using Quantikine® mouse and human VEGF immunoassay kits (R&D Systems, Minneapolis, MN, USA) according to the manufacturer's instructions. Total protein concentration was determined by the BCA protein assay kit (Pierce, Rockford, IL, USA).

In Vitro Studies

MT, VEGF/MT tumors, as well as MT-induced tumors arising in $VEGF^{+/+}$ and $VEGF^{-/-}$ mammary glands were removed aseptically, minced, and seeded in Primaria™ tissue culture flasks (Becton Dickinson, Franklin Lakes, NJ, USA) to suppress fibroblast growth. Tumor cell outgrowths that displayed epithelial morphology, were harvested by trypsinization and cultured on Lab-Tek glass slides (Nalge Nunc International Corp. Naperville, IL, USA) and used at passages 1–3. The cells were fixed in 4% formaldehyde, and incubated with mouse cytokeratin 18 (CK-18) monoclonal antibody (0.5 μg/ml; Chemicon, Temecula, CA, USA) to verify epithelial origin of the tumor cells. To find out if the cultures were contaminated with endothelial cells, they were stained with CD31 antibody (0.5 μg/ml; BD Pharmingen, San Diego, CA, USA). M.O.M. immunodetection kit was used to detect CK-18 and rat CD31anti-mouse monoclonal antibody (BD Pharmingen, San Diego, CA) to detect CD31, followed by the use of the appropriate Vectastain ABC kits and DAB as described above. Flk-1 expression was also examined, using the same mouse monoclonal Flk-1 at 2 μg/ml as described above. Proliferative activity of the MT, VEGF/MT, and $VEGF^{-/-}$ tumor cells was measured using a BrdU cell proliferation ELISA (Roche Diagnostics Corporation, Indianapolis, IN, USA). Total RNA was isolated from semiconfluent cultures of $MT/VEGF^{lox/lox}$ ($VEGF^{+/+}$) and ($MT/VEGF^{-/-}$) tumor cells. A measure of 0.5 μg/ml of RNA were subjected to RT-PCR analysis of CD31, Flk-1, and human VEGF, using the primers listed above. Western blot analysis of Flk-1 expression was carried out on 150 μg of protein lysates from confluent monolayers of passage 1 tumor cells isolated from one MT only tumor and two VEGF/MT tumors, using 40 μg of human dermal microvascular endothelial cells (HDMVEC) as a positive control. PVDF membrane was used for protein transfer and hybridized with Flk-1 antibody (1 μg/ml) (C-1158, Santa Cruz Biotechnology, Santa Cruz, CA, USA). The membranes were then stripped and rehybridized with β-actin**, which served as a loading control. The signal was visualized using HRP-conjugated secondary antibody and the Amersham Pharmacia enhanced chemiluminescence detection system according to the manufacturer's instructions. Western blot analysis was similarly carried out on $p16^{ink4a}$ (p16) and $p21^{WAF1}$ (p21) expression by the $VEGF^{+/+}$ and $VEGF^{-/-}$ tumor cells, using rabbit polyclonal p16 (2 μg/ml) and p21 (2 μg/ml) antibodies from Santa Cruz. Cell cycle analysis was carried out on passage 3 $VEGF^{+/+}$ and $VEGF^{-/-}$ tumor cells. The cells were stained with propidium iodide and subjected to FACS (Becton Dickinson) using Cell Quest 3.2 (Becton Dickinson) software.

Statistics

The data sets for comparison of MT with VEGF/MT were subjected to a two-tailed unpaired t test using GraphPad Prism (GraphPad Software Inc., San Diego, CA, USA). Pearson's correlation was also performed on GraphPad Prism software using either a one-tailed or two-tailed analysis depending upon solid *a priori* knowledge of association. The 0.05 level of probability was used as the minimum criterion of significance for all statistical tests.

Results

VEGF Transgenic Mice Appear Phenotypically Normal

Transgenic $hVEGF_{165}$ was placed into the pSKMMTV-SVPA expression cassette to direct transgene expression to mammary epithelial cells (Figure 1a). Northern blot analysis of transgenic $hVEGF_{165}$ expression was limited to female mice because only females were employed in the present mammary carcinogenesis study. Strong hEGF165 signal was detected in mammary gland and low levels were also observed in the salivary glands, lungs, and spleen (Figure 1b). Expression in those organs was comparable to that reported previously, using the MMTV-LTR promoter to drive expression of a variety of transgenes.[26,31–35] MMTV-VEGF mice described previously showed evidence of VEGF overexpression in the testis and epididymis, that resulted in infertility.[36] However, heterozygous male VEGF mice of the present transgenic model showed no signs of impaired fertility. The dissimilarities between the two MMTV-VEGF mouse models are most likely due to difference in the number and/or location of genomic integration, which are believed to have significant impact on both the level and organ site of transgene expression. Heterozygous female VEGF mice showed no signs of developmental defects, increased morbidity, or impaired reproductive function. Moreover, histological examination of H&E-stained sections of all major organs did not reveal abnormalities. The frequency of spontaneous neoplasia was not higher in the VEGF mice than their WT littermates during a 2-year observation period (data not shown). Measurements of mouse and human VEGF protein levels in the mammary glands showed variable levels at 6 and 8 weeks of age (Figure 1c). There was a significant increase in the median *mu*VEGF protein levels from 6-week-old (90.7 ± 8.1 pg/mg protein) to 8-week-old

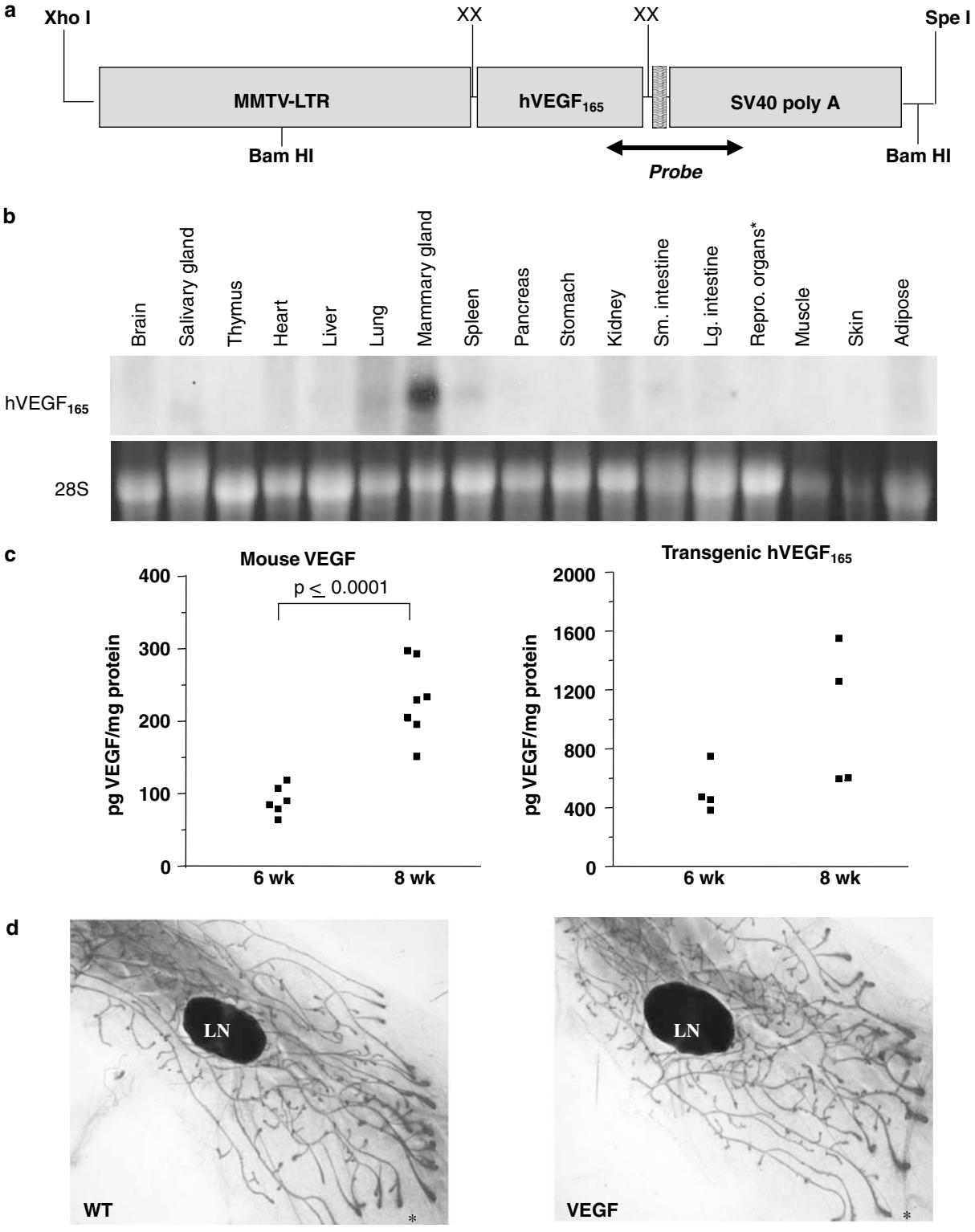

Figure 1 Generation and characterization of MMTV-VEGF mice. (**a**) schematic representation of the MMTV-LTR driven $hVEGF_{165}$ transgene construct. $hVEGF_{165}$ (605 bp), bounded by *Bam*HI restriction sites, was ligated to a *Bgl*II site present in expression vector. The loss of the restriction sites following ligation of *Bam*HI to *Bgl*II is denoted as XX. See Materials and methods for details. Transgene expression levels and tissue specificity were determined by Northern analysis using the 391 bp transgene-derived probe as indicated by the double-ended arrow. (**b**) Multiple-tissue Northern blot analysis of $hVEGF_{165}$ expression in multiple organs of an 8-week-old hemizygous female mouse; 28S band was used as loading control; * reproductive (repro) organs included uterus, uterine horns, and ovaries. (**c**) Endogenous mouse (left panel) and transgenic human $VEGF_{165}$ (right panel) in mammary gland lysates from 6- and 8-week-old female mice. (**d**) Mammary gland whole mounts with lymph nodes (LN) of WT and VEGF mice at 6 weeks of age. Representative proliferating terminal end buds (TEBs) are indicated by *.

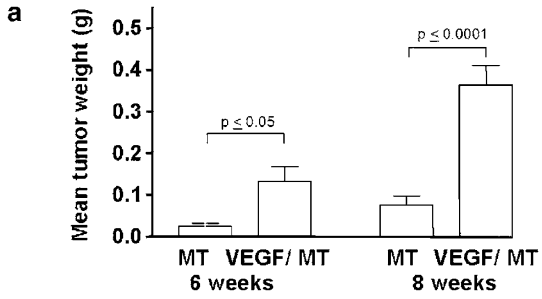

b

	6 weeks		8 weeks	
	MT	VEGF/ MT	MT	VEGF/ MT
number of mice	5	6	8	7
incidence	80%	100%	88%	100%
multiplicity[a]	3.50 ± 0.64	9.33 ± 0.33***	4.20 ± 0.87	9.40± 0.57 **
mean weight(g)[a]	0.02 ± 0.01	0.13 ± 0.03*	0.08 ± 0.02	0.36 ± 0.05***
mean burden (g)[a]	0.11 ± 0.04	1.21 ± 0.30*	0.38 ± 0.09	3.53 ± 0.64***
metastasis (%) [a,b]	0%	33%	0%	100%

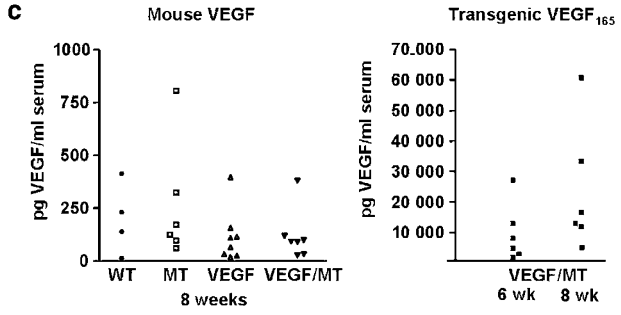

Figure 2 Transgenic $hVEGF_{165}$ expression in mouse mammary epithelial cells results in accelerated development of mammary carcinomas and lung metastases at 6 and 8 weeks of age. (**a**) Mean tumor weight of 6-week-old ($n=5$) and 8-week old ($n=8$) MT mice and 6-week-old ($n=6$) and 8-week-old ($n=7$) VEGF/MT mice. (**b**) Tumor incidence, tumor multiplicity, mean tumor weight, mean tumor burden, and percentage (%) of mice with lung metastases. [a]Represents tumor bearing animals only and [b]represents both micro- and macroscopic lung metastases. Data are shown as means ± s.e. Significant differences between the MT and VEGF/MT groups (*$P\leq0.05$, **$P\leq0.001$, ***$P\leq0.0001$. (**c**) Mouse VEGF serum levels in WT, MT, VEGF, and VEGF/MT mice at 8 weeks of age (left panel). Transgenic $hVEGF_{165}$ serum levels in 6- and 8-week-old VEGF/MT mice (right panel).

(229.9 ± 19.9 pg/mg protein) mice ($P\leq0.0001$). The age-related increase is consistent with the continued branching in the mature virgins due to gonadal hormonal effects on mammary gland development.[37] While a trend toward increasing median transgenic $hVEGF_{165}$ levels was observed from 6-week-old (515.7 ± 80.9 pg/mg protein) to 8-week-old (1004.0 ± 239.7 pg/mg protein) mice, it was not statistically significant. No statistical difference in endogenous mouse VEGF protein levels was detected between the transgenic mice and their WT littermates (data not shown). Since the role of VEGF in mammary development was not the focus of the present study, the analysis was limited to examination of the H&E-stained histological sections and whole mounts of mammary glands obtained from virgin mice at different ages. Microscopic examination revealed no apparent difference in the histology or neovascularization of virgin mammary glands from VEGF and WT mice (not shown). Also, whole mounts of mammary glands from 6-week-old WT and VEGF mice showed comparable number and prominence of the terminal end buds in the developing gland (Figure 1d). It is intriguing that the 5–6-fold increase in total mammary VEGF levels had no apparent effects on mammary gland development of virgin mice or fecundity of dams following multiple round of pregnancies. However, these preliminary developmental studies of virgin mice do by no means rule out that elevated VEGF levels may affect further mammary gland development and function during pregnancy and lactation.

VEGF/MT Mice Display Accelerated Mammary Tumor Growth and Metastatic Development

At 4 weeks of age, palpable mammary tumors were detected in the VEGF/MT mice when only microscopic mammary hyperplasia was observed in the MT littermates. Since palpable tumors were not detectable in the 4-week-old MT mice and the VEGF/MT mice became moribund due to large tumor burden after 8 weeks of age, 6- and 8-week-old tumor-bearing mice were selected for further investigation. The mean tumor weight was significantly greater in the VEGF/MT mice than the MT-only littermates at both 6 weeks (0.13 ± 0.03 g *vs* 0.02 ± 0.01 g; $P\leq0.05$) and 8 weeks of age (0.36 ± 0.05 g *vs* 0.08 ± 0.02g; $P\leq0.0001$) (Figure 2a and b). By 8 weeks of age, 100% of the VEGF/MT mice and 88% of the MT only mice possessed palpable mammary tumors (Figure 2b). The number of tumors per mouse (multiplicity) was significantly higher in the VEGF/MT mice than the MT mice at both 6 weeks (9.33 ± 0.33 *vs* 3.50 ± 0.64; $P\leq0.0001$) and 8 weeks of age (9.40 ± 0.57 *vs* 4.20 ± 0.87; $P=0.0003$). Overall, the mean tumor weight of the VEGF/MT mice was 5.5-fold higher than the MT mice at 6 weeks and 4.5-fold higher at 8 weeks of age. Owing to higher tumor multiplicity and increased mean tumor weight of the VEGF/MT mice, their mean tumor burden was approximately 10- and 9-fold greater at 6 and 8 weeks of age, respectively, than that of the MT-only littermates (Figure 2b). Owing to the high tumor multiplicity in the VEGF/MT mice, we decided to measure mouse and transgenic VEGF in serum of the tumor-bearing mice. This would indirectly assess the total amount of transgenic VEGF produced by the tumors. The mouse VEGF serum levels at 8 weeks of age were unaffected by the presence of the $VEGF_{165}$ and the MT transgene, either individually or in combination and they were variable in all groups (Figure 2c). Interestingly, the highest mouse VEGF (807.9 pg/ml) serum level was detected in a MT-only mouse. This data point appears to be an outlier when compared to other individual values; however, the total tumor

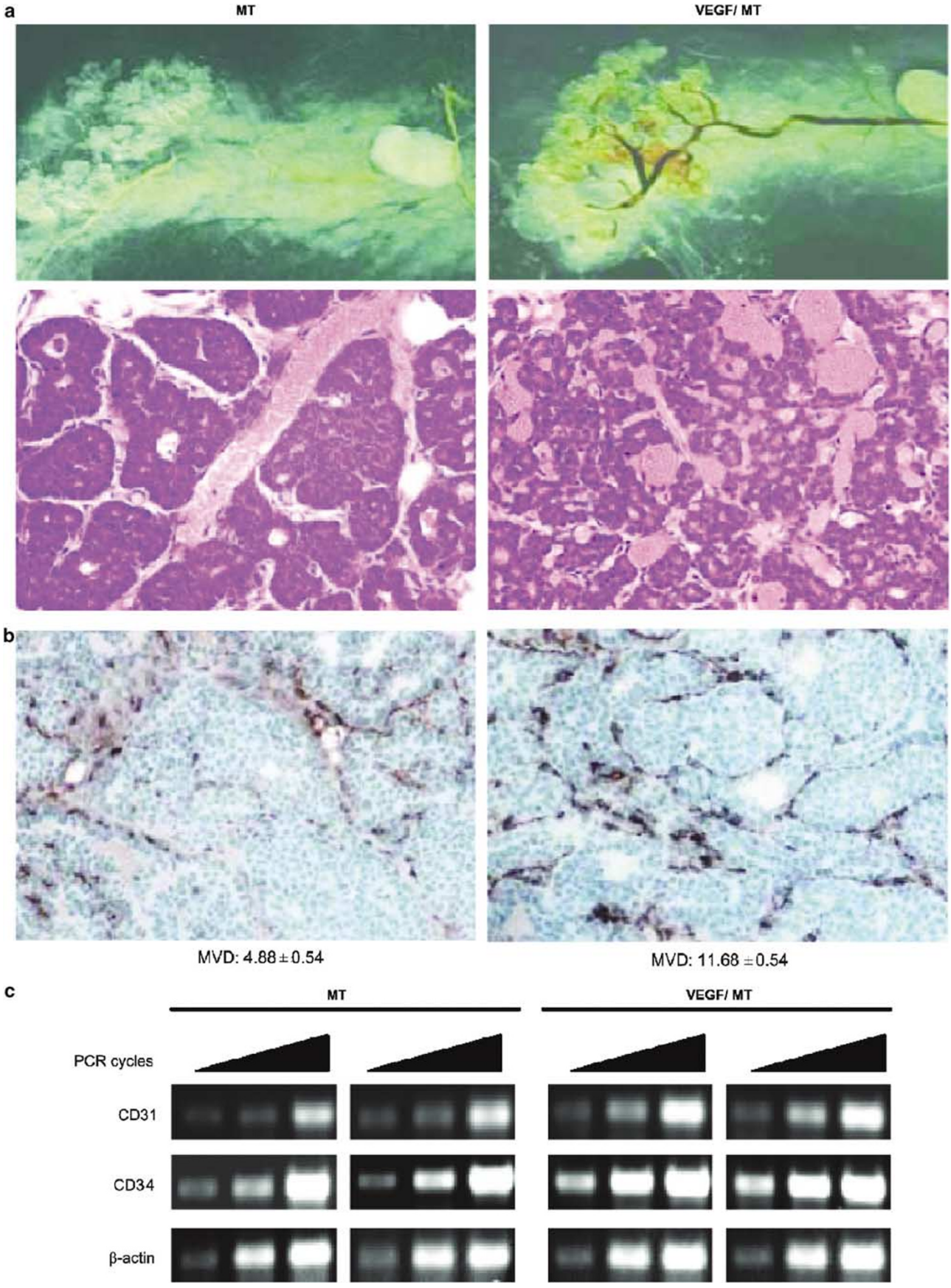
a
MT
VEGF/ MT
b
MVD: 4.88 ± 0.54
MVD: 11.68 ± 0.54
c
MT
VEGF/ MT
PCR cycles
CD31
CD34
β-actin

burden (0.74 g) of this particular mouse was twice that of the mean tumor burden (0.38 g) for MT mice of the same age. As expected, transgenic $hVEGF_{165}$ protein was undetectable in serum by ELISA in the MT-only mice at 8 weeks of age (data not shown). The average serum level of $hVEGF_{165}$ at 8 weeks of age was 892 ± 763 pg/ml in the VEGF mice (Figure 1c), but increased on average 260-fold in tumor bearing VEGF/MT mice (Figure 2c). This presumably reflects the large amount of transgenic $hVEGF_{165}$ released from the tumors into the systemic circulation and it stresses the power of MT to drive transgenic expression in the tumor environment. RT-PCR analysis of transgenic hVEGF expression was carried out on RNA from tumors removed from the R4 and L4 mammary glands of all the animals. Although there was positive correlation between the transgenic hVEGF serum levels and the total tumor burden, a correlation was not found between the VEGF RNA levels and tumor weight of individual tumors (not shown). Since the tumors in the 6- and 8-week-old mice generally occupied the entire mammary glands, it was not possible to compare VEGF expression levels between the tumors and the adjacent non-neoplastic mammary glands. As stated in the Materials and methods section, an attempt to obtain mice with $VEGF^{-/-}$ mammary tumors for tumorigenesis study was unsuccessful because only one tumor-bearing female mouse displayed the $VEGF^{-/-}$ genotype. Nevertheless, the $VEGF^{-/-}$ tumors were useful to evaluate the effects of VEGF gene inactivation on tumor cell apoptosis and growth.

Transgenic $hVEGF_{165}$ had striking accelerating effect on metastatic capability of the MT-induced mammary carcinomas. At 6 weeks of age, 33% of the tumor-bearing VEGF/MT mice had micro- and macroscopic lung metastases, which increased to 100% by 8 weeks of age (Figure 2b). Although MT is known to induce metastatic mammary carcinomas,[26] the 6- and 8-week experimental periods were clearly too short for the development of lung metastases.

Histopathology and Neovascularization of Mammary Carcinomas

Macrosopic tumors were detected only in the VEGF/MT mice at 4 weeks of age. Unstained mammary whole mounts from MT and VEGF/MT mice showed prominent blood-filled vascular tree in the tumor-containing VEGF/MT mammary glands but not the MT-only glands with hyperplastic mammary lesions (Figure 3a, top). H&E-stained sections of the same mammary whole mounts revealed marked vasodilatation in the VEGF/MT tumors (Figure 3a, bottom). This finding suggests that the dilated blood vessels carried increased amount of nutrients and consequently provided growth advantage to the early mammary tumors of the VEGF/MT mice. Microscopic examination of the mammary tumors from 6- and 8-week-old VEFF/MT and MT mice displayed adenocarcinomas with glandular and solid growth patterns as described previously[26] (not shown). The basic growth patterns and differentiation status were comparable in both genotypes but there was more pronounced stroma in the VEGF/MT tumors. Neovascularization was quantitated in CD31-stained frozen tumor sections from 8-week-old VEGF/MT and MT mice. The mean MVD in the VEGF/MT tumors was 11.69 ± 0.54 or 2.4-fold higher than the mean MVD of 4.88 ± 0.54 in the MT-only tumors (Figure 3b). Neovascularization was indirectly assessed by RT-PCR analysis of CD31 and CD34 RNA expression. Using three different numbers of cycles, CD31 was upregulated 68% in the VEGF/MT tumors and CD34, which is more specific for tumor vascular endothelial cells, was upregulated 90% (Figure 3c).

Upregulation of Multiple Angiogenesis-Related Genes in the VEGF/MT Mammary Tumors

To investigate if the elevated VEGF levels and increased MVD were reflected in upregulation of angiogenesis-associated genes, GEArray™ Q series mouse angiogenesis array was carried out on VEGF/MT and MT-only tumors (Table 1). Owing to known variability in transgene expression between any given tumors, the array hybridization was performed with pooled RNA samples (6 per group) and the criteria for significance was set at a 2-fold alteration. Among the 96 genes on the array, 25 genes were differentially expressed, of which 24 were upregulated and one (midkine) was downregulated in the VEGF/MT tumors. Total VEGF expression was increased 3.39-fold in the VEGF/MT tumors but the analysis of mouse VEGF expression was not possible due to the extensive homology between the human VEGF and mouse VEGF cDNA bound to the array. The 3.66-fold increase in RNA expression of

Figure 3 Increased vasodilatation and mean vascular density (MVD) in VEGF/MT tumors. (**a**) Representative unstained mammary gland whole mounts show prominent vascular tree only in the early VEGF/MT mammary tumor at 4 weeks of age ($n = 3$ per group) (upper panels). Representative H&E-stained sections show more prominent microvessels in the VEGF/MT than the MT-only early lesions (lower panels). (**b**) CD31 immunostaining of frozen tumor sections and MVD of the MT and VEGF/MT mammary carcinomas. Blood vessels were counted in ten microscopic fields (magnification $\times 400$) in each of five MT-only tumors and six VEGF/MT tumors; $P < 0.0001$ (Student's *t*-test). (**c**) RT-PCR analysis of two endothelial markers, CD31 and CD34, in representative mammary carcinomas from two 8-week-old MT and two VEGF/MT mice. Triangles indicate increasing cycle numbers for CD31and CD34 (24, 27, 30) and β-actin.[20,23,36] The mean fold increase in gene expression in the VEGF/MT relative to the MT-only tumors after normalization to β-actin was 1.7 for CD31 and 1.9 for CD34.

Table 1 Angiogenesis-related genes upregulated in tumors of VEGF/MT transgenic mice

UniGene	*Genebank*	*Description*	*Gene name*	*Gene/β-actin (optical density)*	*Fold ↑*
Mm.3425	NM 007426	Mus musculus angiopoietin 2 (Agpt2)	angiopoietin 2		1.58
Mm.21767	NM 009868	Mus musculus cadherin 5 (Cdh5),	cadherin 5		4.14
Mm.7978	NM 010109	Mus musculus ephrin A5 (Efna5)	Ephrin A receptor		1.72
Mm.4005	NM 010111	Mus musculus ephrin B2 (Efnb2)	Ephrin B2		1.50
Mm.34533	NM 010144	Mus musculus Eph receptor B4 (Ephb4)	Ephrin B4		1.68
erb-2	U71126	Mus musculus erbB2	erb-2		1.50
Mm.14115	NM_011808	Mus musculus v-ets avian virus E26 oncogene homolog 1 (Ets-1)	c-ets1		1.96
Mm.154768	NM 030614	Mus musculus fibroblast growth factor 16 (Fgf16)	FGF16		1.51
Mm.3157	M33760	Fibroblast growth factor receptor 1	FGFR1 (FLG)		1.61
Mm.4912	NM_008011	Mus musculus fibroblast growth factor receptor 4 (Fgfr4)	FGFR4		1.59
Mm.3879	NM 010431	Mus musculus hypoxia inducible factor 1, alpha subunit (Hif1α)	Hif1α		2.11
Mm.285	X59397	Kinase insert domain protein receptor (Flk-1)	Flk-1		3.11
Mm.4622	NM_009257	Mus musculus serine protease inhibitor 7 (Spi7)	maspin		1.84
Mm.27448	NM 008737	Mus musculus neuropilin (Nrp)	neuropilin		1.98
Mm.12837	NM_008713	Mus musculus nitric oxide synthase 3, endothelial cell (Nos3)	NOS3		1.51
Mm.321	NM_009263	Mus musculus secreted phosphoprotein 1 (Spp1)	osteopontin		2.37
Mm.2822	NM 008816	Mus musculus platelet/endothelial cell adhesion molecule (Pecam)	CD31		3.66
Mm.4809	NM 008827	Mus musculus placental growth factor (Pgf)	PlGF		1.57
Mm.35439	NM 009242	Mus musculus secreted acidic cysteine rich glycoprotein (Sparc)	SPARC		1.50
Mm.1291	M32745	Transforming growth factor, beta 3	TGFβ3		1.97
Mm.197552	D28526	Mus musculus transforming growth factor, beta receptor I (Tgfbr1)	TGFBR1(ALK-5)		1.67
Mm.4345	X73960	Tyrosine kinase receptor 1	Tie1		2.04
Mm.1810	NM 010217	connective tissue growth factor	Tissue factor		3.14
Mm.31540	M95200	Vascular endothelial growth factor	VEGF		3.39

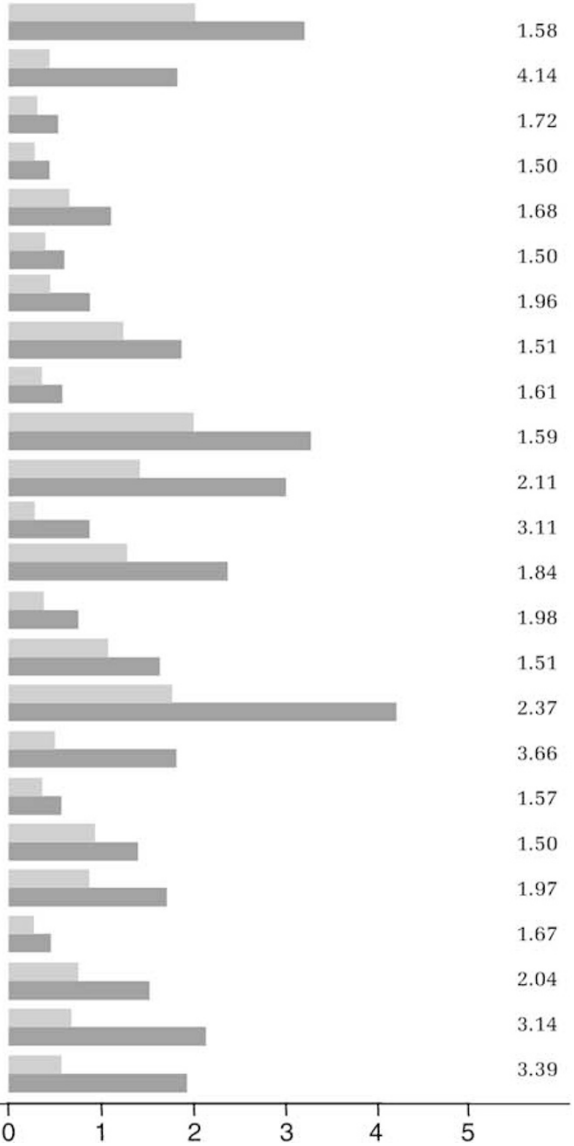

Data derived from GEArray™ Q series mouse angiogenesis array by hybridizing 5 μg of pooled RNA samples ($n = 6$ per group) from MT tumors (light) and VEGF/MT tumors (dark). Analyzed with LumiAnalyst 3.1 and normalized to β-actin.

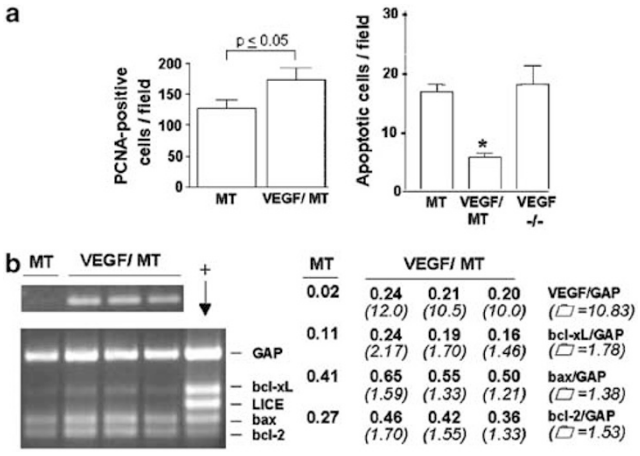

Figure 4 Overexpression of VEGF modulates proliferative and apoptotic activities in mammary tumors. (**a**) The average number of PCNA-positive (left panel) and apoptotic (right panel) tumor cells were determined in nine MT and nine VEGF/MT tumors of 8-week-old mice, as well as three VEGF$^{-/-}$/MT from a 9-month-old mouse. Data represent means$\pm$s.e., *$P\leq0.05$. (**b**) Multiplex RT-PCR of several apoptosis-related genes in one MT and three VEGF/MT mammary tumors (left panel). Gene expression levels after normalization with GAPDH (right panel). The numbers in parentheses represent the fold increase in gene expression in the VEGF/MT tumors relative to the MT tumors.

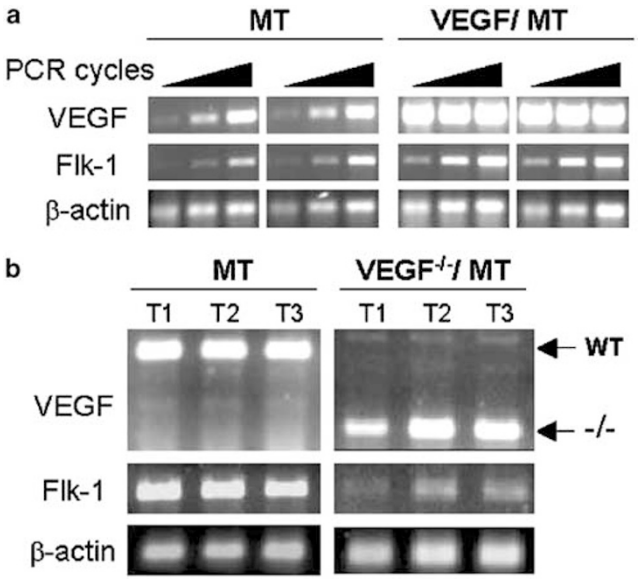

Figure 5 Flk-1 is upregulated in the VEGF/MT tumors and downregulated in VEGF$^{-/-}$ tumors. (**a**) RT-PCR analysis of total VEGF and Flk-1 in representative MT and VEGF/MT tumors from two animals. The triangles indicate increasing numbers of cycles for VEGF and Flk-1[24,27,30] and β-actin.[20,23,30] The mean increase in gene expression in the VEGF/MT tumors after normalization to β-actin was 10.7 for VEGF and 2.0 for Flk-1. (**b**) RT-PCR analysis of VEGF and Flk-1 expression in three (T1–T3) MT and three VEGF$^{-/-}$/MT tumors. The normal mouse VEGF transcript (WT) of the MT only tumors is substituted with a $^{-/-}$ transcript in the VEGF$^{-/-}$/MT tumors, which reflects the Cre-mediated deletion of exon 3 of the VEGF gene. There is a corresponding downregulation of Flk-1.

CD31 in the VEGF/MT tumors is consistent with the higher MVD shown in Figure 3b. Increased expression of the signaling Flk-1 receptor (3.11-fold) in the VEGF/MT tumors was followed up by RT-PCR analysis of individual tumors and Western blot analysis of cultured cells as shown below.

Increased Tumor Cell Proliferation and Survival in the VEGF/MT Tumors

Tumor sections were analyzed for tumor cell proliferative and apoptotic activities. The average number of PCNA-positive tumor cells was significantly higher in the VEGF/MT ($172.0\pm38.9/\times400$ field) than the MT-only tumors (120.6 ± 25.8 cells/$\times400$ field; $P<0.05$) (Figure 4a, left panel). In contrast, the average number of apoptotic tumor cells was significantly lower in the VEGF/MT (5.12 ± 1.98 cells/$\times400$ field) than the MT-only tumors ($16.96\pm6.54/\times400$ field, $P\leq0.005$) (Figure 4a, right panel). The three MT-induced VEGF$^{-/-}$ tumors from the Cre-Lox mouse described in the Material and methods section were employed to examine if the anti-apoptotic effects of the VEGF overexpression were reversed following VEGF gene inactivation. The MMTV-Cre and VEGF-LoxP mouse models have been described previously.[38,39] The Flk-1 binding site is encoded by exon 3 of the VEGF gene, which is excised by the Cre-mediated deletion (Figure 5b) and the autocrine growth stimulatory loop through Flk-1 would be abrogated in the VEGF$^{-/-}$ protein.[40] As expected, the VEGF-mediated cell survival was abolished in the VEGF$^{-/-}$ tumors, which demonstrated similar number of apoptotic cells as the MT-only tumors (Figure 4a, right panel). RT-PCR analysis of hVEGF$_{165}$ and apoptosis-related gene expression revealed upregulation of VEGF, bcl-xL, bax, and bcl-2 in the VEGF/MT tumors (Figure 4b). While not statistically significant when analyzed using a two-tailed Pearson correlation (95% CI), a positive trend was observed between the hVEGF$_{165}$ expression levels and the expression of bcl-xL ($P\leq0.11$), bax ($P\leq0.19$), and bcl-2 ($P\leq0.07$). One-tail analysis showed a significant correlation ($P\leq0.03$) between elevated hVEGF$_{165}$ and upregulation of bcl-2. Consistent with the decreased number of apoptotic cells by immunohistochemistry, the bax/bcl-2 ratio of VEGF overexpressing tumors was nominally lower than the bax/bcl-2 ratio of the MT-only tumors.

Flk-1 Correlates with VEGF Expression in Mammary Tumors

The microarray data revealed upregulation of numerous angiogenesis-associated genes in the VEGF/MT tumors. Further analysis was focused on the signaling VEGF receptor, Flk-1, using the two highest hVEGF-expressing VEGF/MT tumors and two representative MT tumors. Using RT-PCR at three different cycle numbers in the analysis, it was necessary to set the PCR cycles such that endogenous *mu*VEGF in the MT tumors was amplified in a

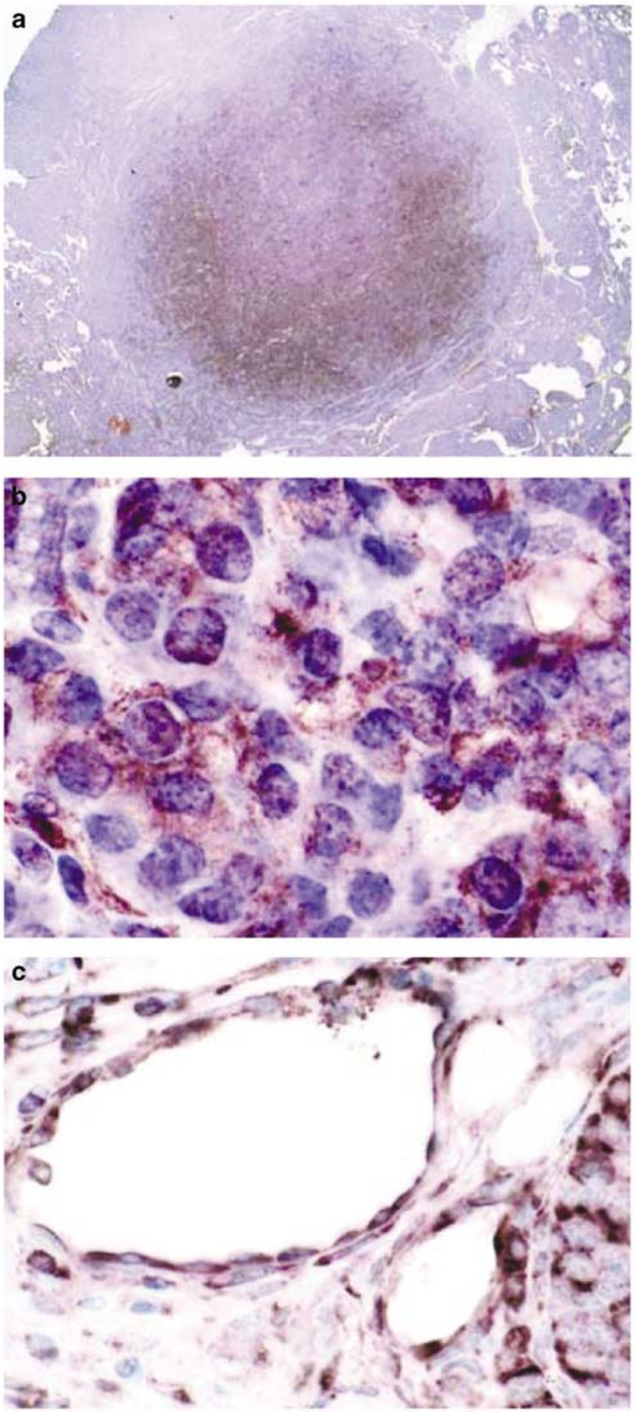

Figure 6 Flk-1 is present in endothelial and tumor cells of the VEGF/MT mammary tumors. Representative tumors show: (**a**) low-power (× 12.5) view of Flk-1-positive nodule with a solid growth pattern; (**b**) high-power (× 400) view of tumor cells of glandular growth pattern showing variable cytoplasmic Flk-1 staining; (**c**) high-power (× 630) view of Flk-1-positive endothelial cells lining blood vessels adjacent to a Flk-1-positive tumor nodule. The data represent four separate immunostaining experiments with similar results. No staining was observed in negative controls (not shown).

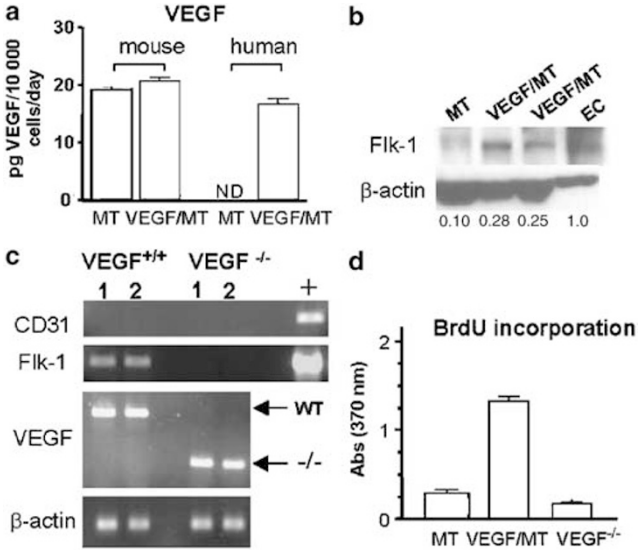

Figure 7 *In vitro* evidence of VEGF-regulated Flk-1 expression and cell proliferation. (**a**) ELISA of mouse and human VEGF levels in culture supernatants of passage one MT and VEGF/MT tumor cells. (**b**) Western blot analysis of Flk-1 expression in passage 1 tumor cells isolated from one MT tumors and two VEGF/MT tumors. Human dermal microvascular endothelial cells (EC) served as a positive control. Lower amount of protein was used from the EC (40 μg) than the tumor cells (150 μg) due to higher endothelial Flk-1 expression. After normalization to β-actin, which was arbitrarily set as 1 for EC, Flk-1 expression of the VEGF/MT cells was 2.5- and 2.8-fold higher than the Flk-1 expression of the MT-only cells and 3–4 times lower than the EC. (**c**) RT-PCR analysis of CD31, Flk-1, and VEGF expression in tumor cells isolated from two $VEGF^{+/+}$ tumors and two $VEGF^{-/-}$ tumors. Cre-mediated excision of exon 3 from the VEGF gene (WT) generated a lower molecular transcript ($^{-/-}$), which was associated with downregulation of Flk-1. + represents the positive CD31 and Flk-1 controls. (**d**) Proliferative activities of passage 1 tumor cells from MT, VEGF/MT, and $VEGF^{-/-}$ tumors. There was markedly enhanced growth of the VEGF overexpressing cells, compared to the MT-only cells, and decreased growth of the $VEGF^{-/-}$ cells. The BrdU ELISA data represent one of three experiments with similar results ($n = 5$, $\pm$s.e.).

logarithmic fashion at the expense of reaching a plateau of hVEGF in the VEGF/MT tumors. The average total VEGF mRNA levels were 10.8-fold higher and Flk-1 2-fold higher in the VEGF/MT tumors than the MT-only tumors (Figure 5a). The $VEGF^{-/-}$ tumors were also examined to find out if Flk-1 was downregulated. To inactivate the VEGF gene, the Flk-1 binding site, which is encoded by exon 3 of the VEGF gene, is excised by the Cre-mediated deletion.[40] As shown in Figure 5b, the Cre-mediated excision of exon 3 of the VEGF gene generated a lower molecular weight transcript in the three $VEGF^{-/-}$ tumors and this was associated with the downregulation of Flk-1. The collective results from the VEGF overexpressing and knockout tumors suggest VEGF-mediated regulation of Flk-1 expression. Since the Flk-1 receptor has been found on tumor cells in human breast cancer,[20] we decided to look for Flk-1 in the VEGF/MT tumors by immunohistochemical analysis. Examples of Flk-1-positive tumor and endothelial cells are depicted in representative VEGF/MT mammary tumors in Figure 6. Uniform FLK-1 staining was observed in the tumor nodules showing solid growth patterns within the

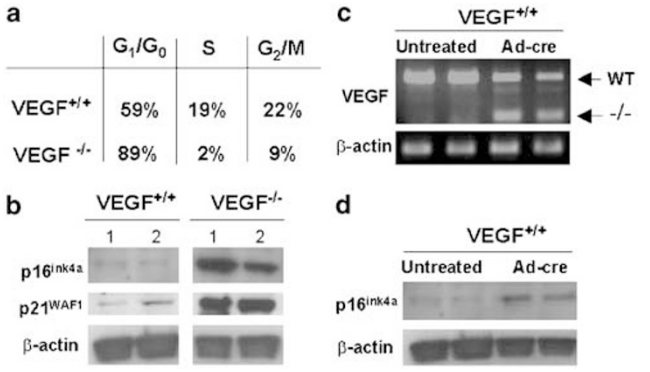

Figure 8 VEGF$^{-/-}$ tumor cells display cell cycle suppression, as well as upregulation of p16 and p21. (**a**) Results from FACS analysis of passage 3 tumor cells isolated from VEGF$^{+/+}$ and VEGF$^{-/-}$ tumors. There is accumulation of the VEGF$^{-/-}$ cells in the G_1/G_0 phase of the cell cycle with a consequent drop in the S and G_2/M phases. (**b**) Western blot analysis shows stimulated p16^{ink4a} (p16) and p21^{WAF1} (p21) expression in the VEGF$^{-/-}$ cells. (**c**) RT-PCR analysis shows partial removal of WT VEGF by Adeno-cre treatment of the VEGF$^{+/+}$ tumor cells. (**d**) Western blot analysis shows stimulation of p16^{ink4a} (p16) following the Adeno-cre treatment.

carcinomas (Figure 6a). However, the intensity of the cytoplasmic Flk-1 staining was more variable in the areas of glandular growth pattern (Figure 6b). Adjacent blood vessels also showed Flk-1 staining of their endothelial lining (Figure 6c).

In Vitro Growth Reflects VEGF and Flk-1 Expression in Tumor Cells

Epithelial outgrowths from MT, VEGF/MT, and VEGF$^{-/-}$ tumor explants were harvested as described in the Materials and methods section and used at passages 1–3 for the *in vitro* experiments. H&E stained passage 1 VEGF/MT cells displayed uniform epithelial-like morphology, which was verified by immunopositivity of the epithelial marker, CK18 (not shown). Staining for endothelial-specific CD31 showed rare (less than 1%) positive cells. Thus, we concluded that the tumor cell cultures used in the *in vitro* studies were minimally contaminated with endothelial cells. In support of the immunohistochemical data, many of the cultured cells were Flk-1 positive (not shown). ELISA of mouse VEGF and transgenic hVEGF released from the passage 1 VEGF/MT and MT tumor cells showed comparable mouse VEGF levels and transgenic hVEGF was produced only by the VEGF/MT as expected (Figure 7a). Interestingly, the VEGF$^{-/-}$ tumor cells at passage 1 displayed flattened morphology, which resembled that of cellular senescence (not shown). Western blot analysis showed 2.5- and 2.8-fold higher Flk-1 expression by the VEGF/MT than the MT-only tumor cells (Figure 7b). This finding, combined with increased MVD, suggested that both EC and tumor cells contributed to the VEGF-mediated increase in Flk-1 RNA levels observed in the VEGF/MT tumors. Nevertheless, the Flk-1 protein levels of the VEGF/MT tumor cells were 3–4 times lower than that expressed by the positive EC control (Figure 7b). RT-PCR analysis of CD31, Flk-1, and VEGF was carried out on RNA from the cultured MT-induced VEGF$^{+/+}$ and VEGF$^{-/-}$ tumor cells (Figure 7c). As was demonstrated in the VEGF$^{-/-}$ tumors (Figure 5a), the cultured tumor cells also expressed the low molecular weight knockout ($^{-/-}$) VEGF transcript. The absence of CD31 transcripts verified that the VEGF$^{-/-}$ tumor cell cultures were not contaminated with EC. Flk-1 was not expressed by the VEGF$^{-/-}$ tumor cells, which suggested that Flk-1 was downregulated following VEGF gene inactivation.

When assessing proliferative activities of the cultured tumor cells at passage 1, there was much higher BrdU uptake by the VEGF/MT than the MT-only cells and the VEGF$^{-/-}$ cells (Figure 7d). This is consistent with the notion that VEGF acts as an autocrine growth factor through Flk-1 in these tumor cells. The growth inhibition displayed by the VEGF$^{-/-}$ tumor cells was further examined by FACS analysis. Consistent with the reduced proliferation rate, 89% of the VEGF$^{-/-}$ tumor cells were accumulated in G_1/G_0 phase of the cell cycle, compared to 59% of the VEGF$^{+/+}$ tumor cells. Consequently, 2% of the VEGF$^{-/-}$ cells were in S phase and 9% in G2/M phase, compared to 19% of the VEGF$^{+/+}$ cells in S phase and 22% in G_2/M phase (Figure 8a). These cell cycle changes were associated with stimulation of the cyclin-dependent kinase (cDk) binding proteins, p16 and p21 (Figure 8b). Further evidence of a link between VEGF gene inactivation and upregulation of p16 was derived from Adeno-cre treatment of the VEGF$^{+/+}$ tumor cells, which showed increased p16 expression following partial elimination of the WT VEGF transcript by Adeno-cre (Figure 8c, d). p21 expression, however, was not affected (not shown).

Discussion

VEGF is overexpressed in primary breast cancer[5,41] and has been identified as an important prognostic determinant in breast cancer.[6] We reported earlier, using a Tet-regulated system, that VEGF is essential for initial but not continued growth of xenografted human breast carcinoma cells, suggesting that VEGF is critical for the early stages of breast cancer development.[42] There is emerging evidence that VEGF receptors are not restricted to vascular endothelial cells and are also present on tumor cells of different types of human malignancies.[20,43,44] *In vitro* studies have suggested that VEGF has an important autocrine function as a survival factor in breast cancer.[45] To the best of our knowledge, the present transgenic model is the first to evaluate the effect of VEGF overexpression at different aspects of mammary tumor development and metastases. The

data indicate that the VEGF employed both blood vessels and tumor cells to promote tumor growth. These involved paracrine effects to increase vasodilatation and neovascularization, and autocrine effects to stimulate tumor cell proliferation and survival.

Different transgenic tumor models have demonstrated higher transgene expression in the malignant than the nonmalignant counterpart.[46–48] We observed very high circulating VEGF levels in the VEGF/MT mice, which possessed 9–10 mammary tumors per mouse. As the entire mammary glands were occupied by the tumors in the 6- and 8-week-old VEGF/MT mice, it was not possible to compare the transgenic VEGF levels in the tumors and the adjacent non-neoplastic mammary tissues. Based on our RNA analysis of inguinal mammary tumors and nonneoplastic mammary glands, transgenic VEGF expression was consistently higher in the tumors (not shown). The variability in transgene expression among the mammary tumors examined may reflect a mosaic transgene expression, which is consistent with previous findings in transgenic mice with MMTV-LTR targeted expression of tetop-LacZ to mammary epithelial cells.[49] In the VEGF/MT tumor group, the high circulating VEGF levels were associated with increased tumor burden. However, there was not a significant correlation between weight and VEGF mRNA levels of individual tumors by statistical analysis. A plausible explanation is that the low VEGF expressing tumors did benefit from the high VEGF expressing tumors, which released large amounts of VEGF into the systemic circulation.

Mammary overexpression of VEGF led to accelerated tumor development in the VEGF/MT mice, which was observed as early as at 4 weeks of age, when the MT littermates displayed only microscopic mammary hyperplasia. The striking vasodilatation in the VEGF/MT tumors at 4 weeks was presumably mediated by VEGF stimulation of the nitric oxide-mediated pathway[50–52] and upregulation of genes like HIF1α, Angiopoietin-2, and Tie1 (Table 1). Additionally, increased endothelial cell proliferation may have contributed to the vasodilatation. It seems reasonable to speculate that vasodilatation results in increased delivery of nutrients to the tumor environment and thus contributes to the early emergence of palpable tumors. Stimulation of the nitric oxide pathway in the VEGF/MT tumors was also demonstrated through upregulation of endothelial nitric oxide synthase-3 by the angiogenesis array (Table 1). The increased amount of stroma in the VEGF/MT tumors can be attributed to the function of VEGF as a vascular permeability factor. As such, VEGF facilitates extravasation of circulating macromolecules such as fibrinogen,[53] fibronectin, vitronectin, and plasminogen,[54] which accumulate in the extravascular compartment and serve as a foundation of tumor stromal formation.[55] Upregulation of endothelial nitric oxide synthase-3 is also important in the signaling events that mediate VEGF-induced vascular hyperpermeability.

The increased MVD in the VEGF/MT tumors was associated with the upregulation of multiple angiogenesis-associated genes detected by the angiogenesis array assay. It is intriguing that the hypoxia-inducible factor-1 alpha (HIF1α) was upregulated in the VEGF/MT tumors. This was suggestive of low oxygen concentration despite the high $hVEGF_{165}$ levels and upregulation of other angiogenic factors. The possibility that a nonhypoxic pathway was responsible for stimulation of HIF1α was not feasible since Angiopoietin-2 and Tie-1 were also upregulated and they are induced by both hypoxia and VEGF.[56,57] The two VEGF receptors that were upregulated in the angiogenesis array were Flk-1 and Nrp-1, a coreceptor of Flk-1.[11] Nrp-1 is induced in cultured endothelial cells following the addition of $hVEGF_{165}$[58] and has also been implicated in human breast carcinoma survival and growth of Nrp-1-transfected AT2.1 rat prostate carcinoma cells *in vivo*.[45,59] Nrp-1 is a downstream target of the Ets-1 transcription factor, which is induced by VEGF[58] and was upregulated in the VEGF/MT tumors. Hence a possible mechanism for increased expression of Nrp-1 in the present model was via VEGF-mediated stimulation of Ets-1.

Earlier documentation of VEGF as an autocrine survival factor for cultured human breast carcinoma cells was recapitulated in our transgenic model through decreased number of apoptotic cells in the VEGF/MT tumors and increased number of apoptotic cells in the $VEGF^{-/-}$ tumors. Admittedly, we did not have sufficient number of tumor-bearing $VEGF^{-/-}$ mice to carry out a carcinogenesis study as stated in the Materials and methods section. Nevertheless, the apoptosis data presented from three tumors of a single $VEGF^{-/-}$ mouse, as well as the *in vitro* data from isolated $VEGF^{-/-}$ tumor cells, provide a powerful complement to the findings obtained from the VEGF overexpressing tumors and tumor cells. Decreased apoptosis in the VEGF overexpressing tumors was associated with upregulation of two antiapoptotic genes, bcl-2 and bcl-xL. Although the proapoptotic gene, bax, was also upregulated, it would not be expected to alleviate the antiapoptotic activity of bcl-2, which is known to be powerful for mammary epithelial cell survival.[60] It has been shown that Flk-1 plays a role in the inhibition of apoptosis.[61] Flk-1 is also a signaling receptor for mitogenic activity of VEGF in endothelial cells and different types of nonendothelial human tumor cells.[20–22] Our *in vitro* demonstration of increased proliferative activity, combined with Flk-1 stimulation of the VEGF/MT tumor cells, presents a circumstantial evidence of an autocrine growth factor function of VEGF and signaling through Flk-1. Further indirect evidence came from the MT-induced $VEGF^{-/-}$ tumor cells, which at passage 1 showed limited replicative potential and

were accumulated in G_1/G_0 phase of the cell cycle. These preliminary findings suggest that VEGF plays a role in the middle T-driven tumor cell proliferation. However, a study on middle T transformed endothelial cells showed that they were not growth affected by inhibition of VEGF signaling.[62] Two *in vivo* studies support a critical role of VEGF at the initial stages of tumorigenesis. First, Shi and Ferrara[63] showed that oncogenic *ras* could not restore tumorigenicity of embryonic stem (ES) cells lacking VEGF. Second, we showed that Tet-regulated suppression of VEGF in T47-D breast carcinoma cells resulted in growth arrest in nude mice.[42] In light of the many potent biological activities of VEGF, it seems reasonable to speculate that VEGF gene inactivation could result in stimulation of other effectors of the cell cycle arrest response. It is also possible that the cell cycle suppression was intensified by the chronic VEGF deficiency in the slow growing mammary carcinomas of the 9-month-old $VEGF^{-/-}$ mouse.

The cell cycle slow-down of the $VEGF^{-/-}$ tumor cells was associated with stimulation of the CDK inhibitors, p16 and p21, which regulate transition between different phases of the cell cycle.[64,65] Increased p16 expression was also observed in the Adeno-cre-treated $VEGF^{+/+}$ tumor cells. These findings suggest that p16 and p21 played a role in the growth inhibition of the $VEGF^{-/-}$ tumor cells. A connection between p16 and VEGF has been reported by showing loss of p16 in association with VEGF expression in squamous cell carcinomas of the esophagus.[66] Also, restoration of WT p16 resulted in VEGF suppression in human glioma cells.[67] It will be important to further characterize the effect of VEGF gene deletion on other cell cycle regulators, including p53, in this transgenic tumor model.

One of the important features of the middle T mammary carcinoma model is the development of lung metastases.[26] There was a striking acceleration of metastatic development associated with VEGF overexpression. When 100% of the VEGF/MT displayed macroscopic lung metastases at 8 weeks, none of the MT-only littermates showed evidence of microscopic lung metastases. This is not surprising in view of the different ways that VEGF may facilitate the metastatic cascade, including the following: increase entry of tumor cells into the circulation through leaky tumor blood vessels; increase survival of tumor cells in the circulation and metastatic cells in the lungs; and stimulate neovascularization of the metastatic colonies in the lungs. Three of the angiogenesis-associated genes that were upregulated in the VEGF/MT tumors and may be linked to metastases were Ets-1, osteopontin, and VE-cadherin. A role for Ets-1 in apoptosis has been established in human endothelial cells[68] and it has also been implicated in activation of metastasis-associated molecules.[58] VEGF stimulates cell migration through a cooperative mechanism involving interaction with $\alpha v\beta 3$ integrin and osteopontin.[69] Osteopontin is a secreted phosphoprotein that is upregulated in a number of human malignancies and is associated with decreased survival in metastatic breast cancer.[70] It was upregulated 2.4-fold and was the highest expressing gene in the VEGF/MT tumors, which may reflect the metastatic capability of this mammary carcinoma model. Cadherin 5, also called VE-cadherin, was overexpressed in the VEGF/MT tumors and may reflect the reported VEGF-stimulated VE-cadherin expression at endothelial adherens junctions.[71]

The VEGF/MT transgenic model is the first to characterize the effects of targeted VEGF overexpression on mammary tumor development and metastases. It provides a powerful complement to previous xenograft models and recapitulates to a surprising degree different biological activities ascribed to VEGF, some of which have been described only through *in vitro* studies. The preliminary *in vitro* data on proliferation and Flk-1 expression of the isolated VEGF overexpressing and $VEGF^{-/-}$ tumor cells strongly suggests that Flk-1 acts as a signaling receptor for the VEGF-stimulated growth. The likelihood that VEGF contributes to tumor progression through both paracrine and autocrine mechanisms in this model is particularly interesting in view of the astonishing results obtained with a humanized VEGF antibody (bevacizumab) in randomized clinical trials in patients with metastatic renal cancer.[72]

Acknowledgements

We thank Dr William J Muller (McMaster University) for providing the MT mice, Dr Napoleone Ferrara (Genentech) for providing the VEGF LoxP mice, and Dr Lothar Hennighausen (NIDDK, NIH) for providing the MMTV-Cre mice. We also thank Dr Giulia Celli and Rick Sharp for valuable technical assistance in making the VEGF transgenic mice.

References

1 Folkman J. Tumor angiogenesis: therapeutic implications. New Engl J Med 1971;285:1182–1186.
2 Folkman J. What is the evidence that tumors are angiogenesis dependent? J Natl Cancer Inst 1990;82: 4–6.
3 Zetter BR. Angiogenesis and tumor metastasis. Annu Rev Med 1998;49:407–424.
4 Weidner N. Tumor angiogenesis: review of current applications in tumor prognostication. Semin Diagn Pathol 1993;10:302–313.
5 Yoshiji H, Gomez DE, Shibuya M, *et al.* Expression of vascular endothelial growth factor, its receptor, and other angiogenic factors in human breast cancer. Cancer Res 1996;56:2013–2016.
6 Obermair A, Kucera E, Mayerhofer K, *et al.* Vascular endothelial growth factor (VEGF) in human breast

cancer: correlation with disease-free survival. Int J Cancer 1997;74:455–458.
7 Senger DR, Galli SJ, Dvorak AM, *et al.* Tumor cells secrete a vascular permeability factor that promotes accumulation of ascites fluid. Science 1983;219: 983–985.
8 Ferrara N, Henzel WJ. Pituitary follicular cells secrete a novel heparin-binding growth factor specific for vascular endothelial cells. Biochem Biophys Res Commun 1989;161:851–858.
9 Alon T, Hemo I, Itin A, *et al.* Vascular endothelial growth factor acts as a survival factor for newly formed retinal vessels and has implications for retinopathy of prematurity. Nat Med 1995;1:1024–1028.
10 Ferrara N, Gerber HP, LeCouter J. The biology of VEGF and its receptors. Nat Med 2003;9:669–676.
11 Soker S, Takashima S, Miao HQ, *et al.* Neuropilin-1 is expressed by endothelial and tumor cells as an isoform-specific receptor for vascular endothelial growth factor. Cell 1998;92:735–745.
12 Carmeliet P, Ferreira V, Breier G, *et al.* Abnormal blood vessel development and lethality in embryos lacking a single VEGF allele. Nature 1996;380:435–439.
13 Fong G-H, Rossant J, Gertsenstein M, *et al.* Role of the Flt-1 receptor tyrosine kinase in regulating the assembly of vascular endothelium. Nature 1995;376: 66–70.
14 Shalaby F, Rossant J, Yamaguchi TP, *et al.* Failure of blood-island formation and vasculogenesis in Flk-1-deficient mice. Nature 1995;376:62–66.
15 Barleon B, Sozzani S, Zhou D, *et al.* Migration of human monocytes in response to vascular endothelial growth factor (VEGF) is mediated via VEGF receptor flt-1. Blood 1996;87:3336–3343.
16 Sondell M, Lundborg G, Kanje M. Vascular endothelial growth factor has neurotrophic activity and stimulates axonal outgrowth, enhancing cell survival and Schwann cell proliferation in the peripheral nervous system. J Neurosci 1999;19:5731–5740.
17 Gerber HP, Vu TH, Ryan AM, *et al.* VEGF couples hypertrophic cartilage remodeling, ossification and angiogenesis during endochondral bone formation. Nat Med 1999;5:623–628.
18 Suzuma K, Takagi H, Otani A, *et al.* Increased expression of KDR/Flk-1 (VEGFR-2) in murine model of ischemia-induced retinal neovascularization. Microvasc Res 1998;56:183–191.
19 Ishida A, Murray J, Saito Y, *et al.* Expression of vascular endothelial growth factor receptors in smooth muscle cells. J Cell Physiol 2001;188:359–368.
20 Kranz A, Mattfeldt T, Waltenberger J. Molecular mediators of tumor angiogenesis: enhanced expression and activation of vascular endothelial growth factor receptor KDR in primary breast cancer. Int J Cancer 1999;84:293–298.
21 Soker S, Kaefer M, Johnson M, *et al.* Vascular endothelial growth factor-mediated autocrine stimulation of prostate tumor cells coincides with progression to a malignant phenotype. Am J Pathol 2001;159: 651–659.
22 Tian X, Song S, Wu J, *et al.* Vascular endothelial growth factor: acting as an autocrine growth factor for human gastric adenocarcinoma cell MGC803. Biochem Biophys Res Commun 2001;286:505–512.
23 Jackson MW, Roberts JS, Heckford SE, *et al.* A potential autocrine role for vascular endothelial growth factor in prostate cancer. Cancer Res 2002;62:854–859.
24 Masood R, Cai J, Zheng T, *et al.* Vascular endothelial growth factor/vascular permeability factor is an autocrine growth factor for AIDS-Kaposi sarcoma. Proc Natl Acad Sci USA 1997;94:979–984.
25 Masood R, Cai J, Zheng T, *et al.* Vascular endothelial growth factor (VEGF) is an autocrine growth factor for VEGF receptor-positive human tumors. Blood 2001;98: 1904–1913.
26 Guy CT, Cardiff RD, Muller WJ. Induction of mammary tumors by expression of polyomavirus middle T oncogene: a transgenic mouse model for metastatic disease. Mol Cell Biol 1992;12:954–961.
27 Maglione JE, Moghanaki D, Young LJ, *et al.* Transgenic Polyoma middle-T mice model premalignant mammary disease. Cancer Res 2001;61:8298–8305.
28 Huang AL, Ostrowski MC, Berard D, *et al.* Glucocorticoid regulation of the Ha-MuSV p21 gene conferred by sequences from mouse mammary tumor virus. Cell 1981;27:245–255.
29 Jhappan C, Stahle C, Harkins RN, *et al.* TGF alpha overexpression in transgenic mice induces liver neoplasia and abnormal development of the mammary gland and pancreas. Cell 1990;61:1137–1146.
30 Kordon EC, McKnight RA, Jhappan C, *et al.* Ectopic TGF beta 1 expression in the secretory mammary epithelium induces early senescence of the epithelial stem cell population. Dev Biol 1995;168:47–61.
31 Berard J, Gaboury L, Landers M, *et al.* Hyperplasia and tumours in lung, breast and other tissues in mice carrying a RAR beta 4-like transgene. EMBO J 1994;13: 5570–5580.
32 Tsukamoto AS, Grosschedl R, Guzman RC, *et al.* Expression of the int-1 gene in transgenic mice is associated with mammary gland hyperplasia and adenocarcinomas in male and female mice. Cell 1998;55:619–625.
33 Matsui Y, Halter SA, Holt JT, *et al.* Development of mammary hyperplasia and neoplasia in MMTV-TGF alpha transgenic mice. Cell 1990;61:1147–1155.
34 Sinn E, Muller W, Pattengale P, *et al.* Coexpression of MMTV/v-Ha-ras and MMTV/c-myc genes in transgenic mice: synergistic action of oncogenes *in vivo*. Cell 1987;49:465–475.
35 Leder A, Pattengale PK, Kuo A, *et al.* Consequences of widespread deregulation of the c-myc gene in transgenic mice: multiple neoplasms and normal development. Cell 1986;45:485–495.
36 Korpelainen EI, Karkkainen MJ, Tenhunen A, *et al.* Overexpression of VEGF in testis and epididymis causes infertility in transgenic mice: evidence for nonendothelial targets for VEGF. J Cell Biol 1998;143: 1705–1712.
37 Hennighausen L, Robinson GW. Think globally, act locally: the making of a mouse mammary gland. Genes Dev 1998;12:449–455.
38 Wagner K-U, Wall RJ, St-Onge L, *et al.* Cre-mediated dene deletion in the mammary gland. Nucelic Acid Res 1997;25:4323–4330.
39 Gerber H-P, Hillan KJ, Ryan AM, *et al.* VEGF is required for growth and survival in neonatal mice. Development 1999;126:1149–1159.
40 Keyt BA, Nguyen HV, Berleau LT, *et al.* Identification of vascular endothelial growth factor determinants for binding KDR and Flt-1 receptors. J Biol Chem 1996; 271:5638–5646.
41 Relf M, LeJeune S, Scott PA, *et al.* Expression of the angiogenic factors vascular endothelial cell growth

factor, acidic and basic fibroblast growth factor, tumor growth factor beta-1, platelet-derived endothelial cell growth factor, placenta growth factor, and pleiotrophin in human primary breast cancer and its relation to angiogenesis. Cancer Res 1997;57:963–969.
42 Yoshiji H, Harris SR, Thorgeirsson UP. Vascular endothelial growth factor/vascular permeability factor is essential for initial but not continued *in vivo* growth of human breast carcinoma cells. Cancer Res 1997;57: 3924–3928.
43 Nakopoulou L, Stefanaki K, Panayotopoulou E, *et al.* Expression of the vascular endothelial growth factor receptor-2/Flk-1 in breast carcinomas: correlation with proliferation. Hum Pathol 2002;33:863–870.
44 Stewart M, Turley H, Cook N, *et al.* The angiogenic receptor KDR is widely distributed in human tissues and tumours and relocates intracellularly on phosphorylation. An immunohistochemical study. Histopathology 2003;43:33–39.
45 Bachelder RE, Crago A, Chung J, *et al.* Vascular endothelial growth factor is an autocrine survival factor for neuropilin-expressing breast carcinoma cells. Cancer Res 2001;61:5736–5740.
46 Kitsberg DI, Leder P. Keratinocyte growth factor induces mammary and prostatic hyperplasia and mammary adenocarcinoma in transgenic mice. Oncogene 1996;13:2507–2515.
47 Krane IM, Leder P. DF/heregulin induces persistence of terminal end buds and adenocarcinomas in the mammary glands of transgenic mice. Oncogene 1996; 12:1781–1788.
48 Cardiff RD, Muller WJ. Transgenic mouse models of mammary tumorigenesis. Cancer Surv 1993;16:97–113.
49 Hennighausen L, Wall RJ, Tillmann U, *et al.* Conditional gene expression in secretory tissues and skin of transgenic mice using the MMTV-LTR and tetracycline responsive system. J Cell Biochem 1995;59: 463–472.
50 Fukumura D, Gohongi T, Kadambi A, *et al.* Predominant role of endothelial nitric oxide synthase in vascular endothelial growth factor-induced angiogenesis and vascular permeability. Proc Natl Acad Sci USA 2001;98:2604–2609.
51 Yamashita T, Kawashima S, Ozaki M, *et al.* Role of endogenous nitric oxide generation in the regulation of vascular tone and reactivity in small vessels as investigated in transgenic mice using synchrotron radiation microangiography. Nitric Oxide 2001;5:494–503.
52 Harris SR, Schoeffner DJ, Yoshiji H, *et al.* Tumor growth enhancing effects of vascular endothelial growth factor are associated with increased nitric oxide synthase activity and inhibition of apoptosis in human breast carcinoma xenografts. Cancer Lett 2002;179:95–101.
53 Dvorak HF, Senger DR, Dvorak AM, *et al.* Regulation of extravascular coagulation by microvascular permeability. Science 1985;227:1059–1061.
54 Senger DR. Molecular framework for angiogenesis: a complex web of interactions between extravasated plasma proteins and endothelial cell proteins induced by angiogenic cytokines. Am J Pathol 1996;149:1–7.
55 Brown LF, Guidi AJ, Schnitt SJ, *et al.* Vascular stroma formation in carcinoma *in situ*, invasive carcinoma, and metastatic carcinoma of the breast. Clin Cancer Res 1999;5:1041–1056.
56 McCarthy MJ, Crowther M, Bell PR, *et al.* The endothelial receptor tyrosine kinase tie-1 is upregulated by hypoxia and vascular endothelial growth factor. FEBS Lett 1998;423:334–338.
57 Oh H, Takagi H, Suzuma K, *et al.* Hypoxia and vascular endothelial growth factor selectively up-regulate angiopoietin-2 in bovine microvascular endothelial cells. J Biol Chem 1999;274:15732–15739.
58 Oh H, Takagi H, Otani A, *et al.* Selective induction of neuropilin-1 by vascular endothelial growth factor (VEGF): a mechanism contributing to VEGF-induced angiogenesis. Proc Natl Acad Sci USA 2002;99: 383–388.
59 Miao HQ, Lee P, Lin H, *et al.* Neuropilin-1 expression by tumor cells promotes tumor angiogenesis and progression. FASEB J 2000;14:2532–2539.
60 Schorr K, Li M, Bar-Peled U, *et al.* Gain of Bcl-2 is more potent than bax loss in regulating mammary epithelial cell survival *in vivo*. Cancer Res 1999;59:2541–2560.
61 Shaheen RM, Tseng WW, Vellagas R, *et al.* Effects of an antibody to vascular endothelial growth factor receptor-2 on survival, tumor vascularity, and apoptosis in a mureine model of carcinomatosis. Int J Oncol 2001; 18:221–226.
62 Muhlner U, Mohle-Steinlein U, Wizigmann-Voos S, *et al.* Formation of transformed endothelial cells in the absence of VEGFR-2/Flk-1 by polyoma middle T oncogene. Oncogene 1999;18:4200–4210.
63 Shi YP, Ferrara N. Oncogenic ras fails to restore an *in vivo* tumorigenic phenotype in embryonic stem cells lacking vascular endothelial growth factor (VEGF). Biochem Biophys Res Commun 1999;254:480–483.
64 Macip S, Igarashi M, Fang L, *et al.* Inhibition of p21-mediated ROS accumulation can rescue p21-induced senescence. EMBO J 2002;21:2180–2188.
65 Yaswen P, Stampfer M. Molecular changes accompanying senescence and immortalization of cultured human mammary epithelial cells. Int J Biochem Cell Biol 2002;34:1382–1394.
66 Takeuchi H, Ozawa S, Shih CH, *et al.* Loss of p16INK4a expression is associated with vascular endothelial growth factor expression in squamous cell carcinoma of the esophagus. Int J Cancer 2004;109:483–490.
67 Harada H, Nakagawa K, Iwata S, *et al.* Restoration of wild-type p16 down-regulates vascular endothelial growth factor expression and inhibits angiogenesis in human gliomas. Cancer Res 1999;59:3783–3789.
68 Teruyama K, Abe M, Nakano T, *et al.* Role of transcription factor Ets-1 in the apoptosis of human vascular endothelial cells. J Cell Physiol 2001;188: 243–252.
69 Senger DR, Ledbetter SR, Claffey KP, *et al.* Stimulation of endothelial cell migration by vascular permeability factor/vascular endothelial growth factor through cooperative mechanisms involving the alphavbeta3 integrin, osteopontin, and thrombin. Am J Pathol 1996;149:293–305.
70 Singhal H, Bautista DS, Tonkin KS, *et al.* Elevated plasma osteopontin in metastatic breast cancer associated with increased tumor burden and decreased survival. Clin Cancer Res 1997;3:605–611.
71 Esser S, Lampugnani MG, Corada M, *et al.* Vascular endothelial growth factor induces VE-cadherin tyrosine phosphorylation in endothelial cells. J Cell Sci 1998;111, (Part 13) 1853–1865.
72 Yang JC, Haworth L, Sherry RM, *et al.* A randomized trial of bevacizumab, an anti-vascular endothelial growth factor antibody, for metastatic renal cancer. N Eng J Med 2003;349:427–437.